# Capture-SELEX of DNA Aptamers for Estradiol Specifically and Estrogenic Compounds Collectively

Chenqi Niu[1,2], Chong Zhang[1*] and Juewen Liu[2*]

[1]MOE Key Laboratory for Industrial Biocatalysis, Institute of Biochemical Engineering, Department of Chemical Engineering, Tsinghua University, Beijing, 100084, China

E-mail: chongzhang@mail.tsinghua.edu.cn

[2]Department of Chemistry, Waterloo Institute for Nanotechnology, Water Institute, University of Waterloo, 200 University Avenue West, Waterloo, Ontario N2L 3G1, Canada

E-mail: liujw@uwaterloo.ca

## Abstract

Estrogenic compounds such as estrone (E1), 17β-estradiol (E2), and 17α-ethynylestradiol (EE2) are serious environmental contaminants due to their potent biological activities. At least six selections were previously reported to obtain DNA aptamers for E2, highlighting its environmental importance. A careful analysis revealed that the previous aptamers are either too long or do not bind optimally. Herein, a series of new aptamers were obtained from the capture-SELEX method with dissociation constants down to 30 nM as determined by isothermal titration calorimetry (ITC). Two aptamers were converted to structure-switching fluorescent biosensors, which achieved limit of detection down to 3.3 nM and 9.1 nM E2, respectively. One aptamer showed similar binding affinities to all the three estrogens, while the other aptamer is more selective for E2. Both aptamers required $Mg^{2+}$ for binding. The proposed sensors were successfully applied in the determination of E2 in wastewater. Moreover, comparisons were made with previous aptamers based on primary sequence alignment and secondary structures. Among previously reported truncated aptamers, ITC showed binding only in one of them. The newly selected aptamers have the combined advantages of small size and high affinities.

**Keywords:** estrogens; aptamers; water; biosensors; environmental monitoring

**Synopsis**: A group of short DNA aptamers were selected to monitor 17β-estradiol and related estrogens individually and collectively in environmental water samples, demonstrating comparative advantages to previously reported aptamers.

## Introduction

17β-estradiol (E2) is a natural estrogen steroid and a major female sex hormone. It is a key regulator of growth, differentiation, and function in a wide range of tissues, including the reproductive system, mammary glands, skeletal system, and cardiovascular system.[1] Some closely related compounds include natural estrone (E1) and synthetic 17α-ethynylestradiol (EE2), which is the active component of contraceptive pills.

Estrogen hormones and their metabolites have emerged as a serious environmental problem due to their overuse in medicine and livestock farming.[2, 3] A seven-year study on an experimental lake area in northwestern Ontario, Canada, showed that chronic exposure to low levels (ng/L) of EE2 had led to the production of vitellogenin mRNA and protein. This in turn caused the feminization of male fish and ultimately led to the extinction of the species from the lake.[4] To manage this environmental problem, a highly reliable, convenient and sensitive analytical method of E2, as well as other estrogenic compounds such as E1 and EE2 is required.

The current methods for the detection of E2 include HPLC-MS[5] and GC-MS.[6] However, these techniques need expensive instrumentation, intricate sample pre-treatment and skilled technicians. Furthermore, they are available only in centralized labs thus disallowing onsite detection. In recent years, various biosensors have been developed for the measurement of E2, including electrochemistry,[7-9] fluorescence,[10, 11] and colorimetry.[12-14] In addition, sensors involving nanomaterials have also been reported.[15-18]

Aptamers are single-stranded oligonucleotides selected to bind target molecules. Compared to antibodies, DNA aptamers offer a number of advantages such as programmable structures, more stable and more cost-effective making them highly attractive for the detection of E2.[19-21] While immunoassays for E2 have been developed, they need to be carried out in a competitive assay format (i.e. signal-off sensors).[22] With site-specific labeling and programmability, aptamers can be coupled with various signaling platforms for signal-on detection of small molecules in environmental samples.[23] In fact, E2 is probably the most popular target for the selection of DNA aptamers with at least six different labs reporting it. The first E2 aptamer was reported by the Gu group in 2007.[24] This 76-mer aptamer ($K_d$ 130 nM) has been used in many sensors in its full-length,[25, 26] and little efforts were made to truncate it.[27] In 2014, the Hodgkiss group reported a 75-

mer DNA aptamer.[28] Based on the intrinsic fluorescence of E2 and a filtration assay, the $K_d$ was determined to be 50 nM. In 2015, using a gold nanoparticle (AuNP) assay, this aptamer was truncated from 75-mer to 35-mer (14 nM $K_d$) and 22-mer (11 nM $K_d$).[29] In 2015, Vanschoenbeek et al reported a series of E2 aptamers using different negative selection targets, but most of the aptamers have $K_d$ around 10 μM.[30] In 2015, the Silverman group selected an aptamer named E2Apt1 with a $K_d$ of 0.6 μM measured by dimethylsulphate (DMS) footprinting.[31] In 2019, in a one-pot selection work for multiple steroids, an 89-mer aptamer named E28 was reported with $K_d$ ranged from 2.2 nM to 15.2 nM E2.[32]

The abovementioned five aptamers were isolated by immobilization of target molecules. In 2012, using the library immobilization method, the Stojanovic lab selected an aptamer for E2 named BES.1.[33] The DNA library was pre-structured to fold in a three-way junction and contained only eight randomized nucleotides, which may not achieve the best aptamers.[34] Aside from these six DNA aptamer selections, there are also RNA aptamers for E2.[35] While these aptamers are quite different in length, sequence, and predicted secondary structure, they have been extensively used to detect E2 in various biosensors.[36-40]

After reading the literature and our own experiments, we found that the current aptamers were either used in their full length (little effort made in truncation) or showed poor or no binding (*vide infra*). Therefore, short, high affinity DNA aptamers for E2 are still needed. Herein, we performed a new selection by immobilizing a fully randomized DNA library, which was never performed before for E2. A few new aptamers were obtained with low nM affinities, two of which were designed in fluorescent biosensors for the detection of E2 in wastewater. Finally, we also compared a few truncated aptamers for binding to E2.

## Materials and Methods

### Chemicals

The DNA samples used in this study were purchased from Integrated DNA Technologies (Coralville, IA, USA, see Table S1 for sequences). Streptavidin agarose resin was purchased from Fisher Scientific. 17β-Estradiol (E2), estrone (E1), 17α-ethynylestradiol (EE2), deoxycholic acid, cortisol, thymidine, dopamine, sodium chloride, magnesium chloride, sodium hydroxide,

hydrochloric acid, tris(hydroxymethyl)aminomethane, and Amicon Ultra-0.5 centrifugal filter unit (3k and 10k molecular weight cut off) were purchased from Millipore-Sigma (Oakville, ON, Canada). 4-(2-Hydroxyethyl) piperazine-1-ethanesulfonic acid (HEPES) and its sodium salt form were purchased from Biobasic Inc. (Markham, ON, Canada). SsoFast EvaGreen supermix was from Bio-Rad. dNTP mix, Taq DNA polymerase with ThermoPol buffer, and the low molecular weight DNA ladder were purchased from New England Biolabs (Ipswich, MA, USA). All buffers and solutions were prepared with Milli-Q water.

**Buffers**

*SELEX buffer*: 20 mM Tris, pH 7.4, 500 mM NaCl, 10 mM $MgCl_2$. *Strand separation buffer*: 20 mM Tris, pH 7.4, 250 mM NaCl. *Sensing buffer*: 20 mM HEPES, pH 7.4, 100 mM NaCl, 10 mM $MgCl_2$. *$Mg^{2+}$-free sensing buffer*: 20 mM HEPES, pH 7.4, 100 mM NaCl. *$Na^+$-free sensing buffer*: 20 mM HEPES, pH 7.4, 10 mM $MgCl_2$. *E09 buffer*: 100 mM Tris-HCl, pH 8.0, 200 mM NaCl, 10 mM $MgCl_2$, 25 mM KCl, 5% ethanol.[24] *22-mer-truncated-H buffer*: 2 mM HEPES, pH 7.5, 10 mM NaCl, 0.2 mM $MgCl_2$, 0.5 mM KCl, 0.1 mM $CaCl_2$, 5% ethanol.[29] *BES.1 buffer*: 20 mM Tris, pH 7.4, 1 M NaCl, 10 mM $MgCl_2$.[33]

**SELEX for E2**

The aptamer selection method was based on previous reports of the Stojanovic group with slight modifications.[41] For each round of selection, the single-stranded DNA library (500 pmol) was first annealed with biotinylated capture strand (2500 pmol) in 250 µL SELEX buffer followed by a slow cooling to room temperature. Meanwhile, 250 µL of streptavidin agarose resin was transferred into a column and washed five times with 500 µL of the SELEX buffer. The annealed DNA was then repeatedly cycled through the streptavidin agarose resin and washed 12 times with 500 µL of SELEX buffer. After washing, 250 µL of E2 solution was cycled through 3 times and the eluted DNA was collected (total 750 µL). The collected eluent was further concentrated and purified with Milli-Q water using a 3k centrifugal filter. The final volume of the purified DNA was adjusted to 60 µL using Milli-Q water. PCR was then performed to obtain 2 mL of amplicon using the biotinylated reverse primer, which was further concentrated and purified with the strand separation buffer using a 10k centrifugal filter. After loading the purified PCR product onto a column and washed 10 times with 500 µL of strand separation buffer, 600 µL of 0.2 M NaOH was added and the eluted ssDNA library was neutralized with HCl. Finally, the library was washed 4

times with Milli-Q water and washed 2 times with strand separation buffer in a 3k centrifugal filter. The purified library was dissolved in 55 μL strand separation buffer and quantified using a Spark microplate reader (Tecan). The amount of library used in each round is shown in Table S2. The PCR product of the round 8, 9, 11 and 12 libraries were sequenced by the Illumina method as described previously.[42] Sequencing results were analyzed with Geneious Prime and Clustal Omega.

**Isothermal titration calorimetry (ITC)**

ITC was performed using a VP-ITC microcalorimeter instrument (MicroCal) following previously reported procedures.[43] Prior to each measurement, all of the solutions were degassed for 5 min to remove air bubbles. DNA aptamer (5 μM) in buffer was loaded in the ITC cell (1.45 mL) at 25°C. E2 (100 μM) in the same buffer was titrated (20 μL each time) into the cell through a syringe, except for the first injection (2 μL). For the BES.1 aptamer, the combination of 10 μM aptamer and 400 μM E2 was used. The enthalpy ($\Delta H$) and association constant $K_a$ were obtained by fitting the titration curves to a one-site binding model using the Origin software. Sensing buffer was used for aptamer CN-Es1, CN-Es2 and CN-Es3. The E09 buffer was used for aptamer E09. The 22-mer-H buffer was used for aptamer 22-mer-H, and the BES.1 buffer was used for aptamer BES.1.

**Detection in buffer**

FAM-labeled E2 aptamer (1 μM FAM-CN-Es1 or FAM-CN-Es2) or FAM-labeled adenosine aptamer was annealed with 2 μM quencher-labeled strand in the sensing buffer to obtain sensor complex stocks. Typically, the sensor reaction contained 20 nM sensor complex in 98 μL sensing buffer. The background fluorescence signal was monitored for 5 min. Then, 2 μL E2 of various concentrations was added. The signal kinetics were continuously monitored for 20 min (excitation at 485 nm; emission at 520 nm). For the specificity experiment, the final concentrations of E2 and other molecules were 2 μM. In the specificity test of the two biosensors for E2, the $F/F_0$ values were used to indicate the sensor response, where F is the fluorescence signal in the presence of a target and $F_0$ is the fluorescence signal before adding the target.

**Detection in real samples**

The wastewater sample was collected from Kitchener, ON, Canada. After allowing the water samples to stand still in a fridge for 24 h, the supernatant was collected and the sensing buffer was added. Then, 10 μL of 40 μM, 20 μM, 10 μM, 7.5 μM, 5 μM and 1 μM E2 were added into 1 mL

wastewater samples to prepare 400 nM to 10 nM E2 in sensing buffer, respectively (final wastewater in the sensor sample was 99%). FAM-labeled E2 aptamers were annealed as described above in the sensing buffer. For the detection of E2 in wastewater, the 1 μL of 10 μM sensor complex stock was added into 100 μL buffered wastewater (final sensor 100 nM) containing various concentrations of E2. Then, the fluorescence signal was collected (excitation at 485 nm; emission at 520 nm). For the specificity experiment in wastewater, the final concentrations of E2, E1 and EE2 were 200 nM.

## Results and Discussion

### Capture-SELEX for E2

In this work, we used the capture-SELEX method[42, 44-47] by immobilization of a library with a 30-nucleotide random region (N30) via hybridization. The N30 region was fully randomized and the two flanking constant primer binding regions can fold the library into an overall stem-loop structure (see Table S1 for DNA sequences). A scheme of the selection method is shown in Figure S1. The E2 concentration was gradually decreased from 100 μM to 5 μM during the 12 rounds of selection (see Table S2 for the selection conditions). We used real-time PCR to monitor the concentration of eluted DNA and thus the progress of the selection (Figure S2). Initially, the difference of the PCR cycles to emerge fluorescence signal (Ct value) between washing the immobilized library with buffer and with E2 was close to zero. After 6 rounds of selection, the difference gradually increased and reached 5 cycles for the last three rounds, suggesting the enrichment of aptamers.

Finally, the round 8, 9, 11 and 12 libraries were sequenced. For round 12, out of a total of 50728 sequences obtained, we analyzed the top 20 most abundant sequences (named CN-Es1 to CN-Es20 respectively) and they can be divided into three major families along with some other sequences (Figure 1). CN-Es1 and CN-Es13 comprised the most abundant family 1 and they have circular permutation sequences, which are typical for small molecular binding aptamers.[48, 49] Families 2 and 3 also have long stretches of conserved nucleotides. We analyzed the percentage of the five most abundant sequences in round 12 and their presence in the other rounds (Table S3).

Interestingly, the first 4 sequences all gradually increased by at least 10-fold from round 8 to round 12. The change in abundance suggested the enrichment of aptamers with high affinities.

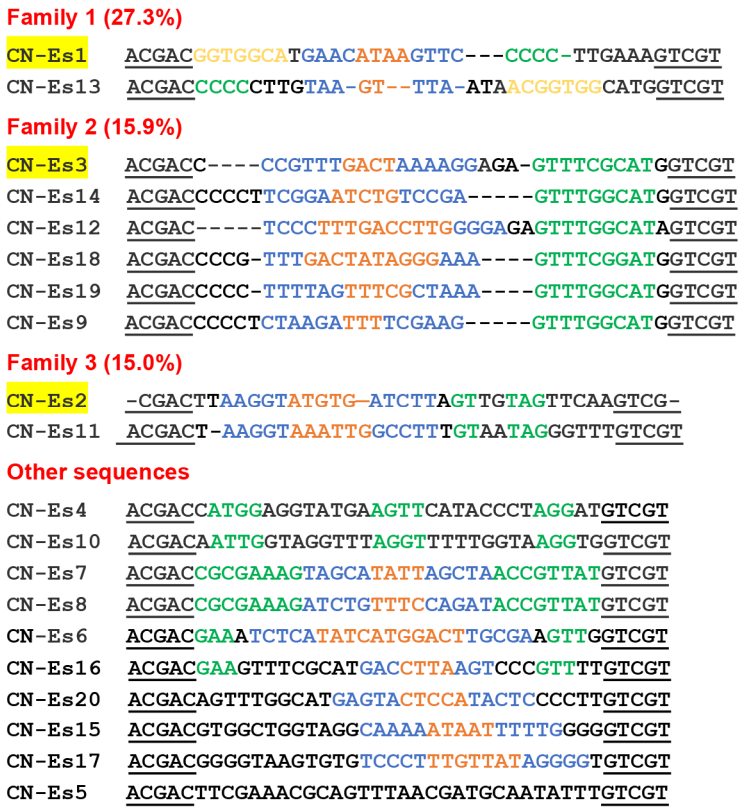



**Figure 1**. Alignment of the top 20 aptamer sequences in the round 12 library. The nucleotides from the primer-binding regions are in underline. Conserved sequences are shown in green and yellow, and hairpin structures are shown in blue and orange. The percentages of sequences in each family are out of a total of 50728 sequences. The most abundant sequence in each family highlighted in yellow was tested experimentally.

## High affinity aptamers for E2

The secondary structures of the top three sequences (belong to three different families) predicted by Nupack are shown in Figure 2A-2C, and they all possess a bulged two-way junction structure. To measure aptamer binding, we performed isothermal titration calorimetry (ITC) by titrating 100 μM E2 into 5 μM aptamers, and the rate of heat released was recorded (Figure 2D-F, top panels).

All the reactions were exothermic as indicated by the downward spikes of the thermograms and the net heat was integrated and fitted to a one-site binding model (Figure 2D-F, lower panels). The $K_d$ was calculated to be 83 ± 25 nM for CN-Es1, 30 ± 14 nM for CN-Es2 and 157 ± 39 nM for CN-Es3. Such affinities are comparable with aptamers binding to other steroids such as testosterone (80 nM) and cortisol (30-140 nM).[34] For the subsequent studies, we focused on CN-Es1 and CN-Es2 since they have lower $K_d$.

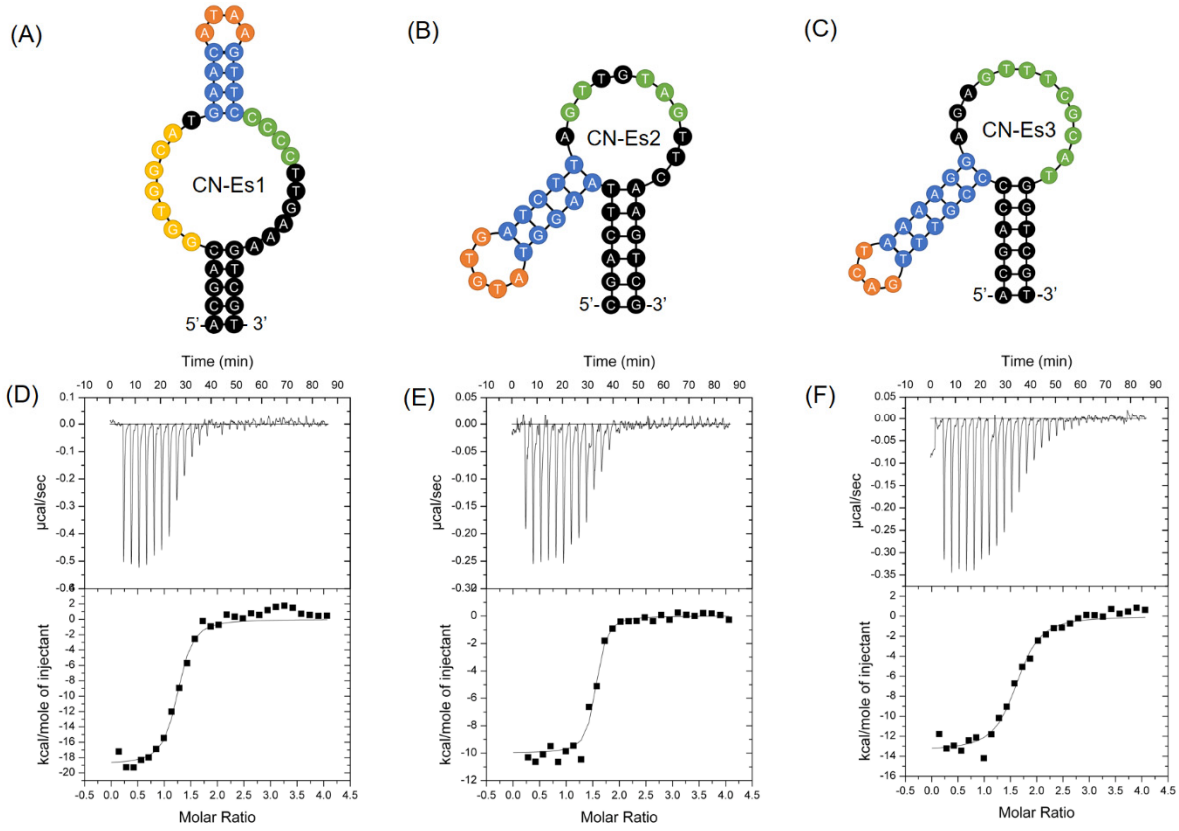



**Figure 2**. The secondary structures of the three aptamers: (A) CN-Es1, (B) CN-Es2, and (C) CN-Es3. The conserved regions based on primary sequence alignment are shown in green and yellow, and the hairpin structures are shown in blue and orange. The ITC data of titrating 100 µM E2 into 5 µM (D) CN-Es1, (E) CN-Es2, and (F) CN-Es3.

The thermodynamic values from the ITC data are listed in Table 1. All the three tested aptamers had large negative $\Delta H$ values, whereas their $\Delta S$ values were negative or close to zero. Therefore, their binding was dominated by the enthalpy term. For aptamers with more heat released, the

entropy decrease was also larger, leading to similar $K_d$ values. This entropy-enthalpy compensation can be explained by tighter binding (more negative enthalpy) accompanied with less freedom of motion (more entropy loss). It is interesting to note that the entropy term was quite different for these three aptamers, implying that these aptamers bind to E2 via different ways, which is consistent with their belonging to different families.

**Table 1**. The thermodynamic values of the ITC experiments.

| Aptamer | Stoichiometry ($N$) | $K_d$ (nM) | $\Delta H$ (kcal/mol) | $\Delta S$ (cal/K/mol) |
|---|---|---|---|---|
| CN-Es1 | 1.20 ± 0.02 | 83 ± 25 | -18.9 ± 0.5 | -30.9 |
| CN-Es2 | 1.50 ± 0.02 | 30 ± 14 | -10.0 ± 0.3 | 0.9 |
| CN-Es3 | 1.58 ± 0.03 | 157 ± 39 | -13.4 ± 0.4 | -14.0 |
| BES.1 | 2.6 ± 0.1 | 1105 ± 407 | -1.9 ± 0.1 | 20.9 |

## Fluorescent Sensing of E2

After confirming the strong binding affinities of our aptamers, we then developed biosensors based on aptamer CN-Es1 and CN-Es2 to detect E2 using the strand displacement method.[21, 50, 51] We extended the aptamer strands by a few nucleotides (the orange regions in Figure 3A or Figure 3D) and labeled a FAM fluorophore. Then, a 12-mer DNA with a quencher label was hybridized to quench the fluorescence. In the presence of E2, the aptamers would bind to E2, form a hairpin structure, and release the quencher-labeled strand, resulting in a fluorescence increase.[50] The ratio of the fluorophore-labeled and quencher-labeled strands was 1:2 to achieve a low background.

Different concentrations of E2 ranging from 2 nM to 50 μM were added to evaluate the sensitivity. When E2 was added, the fluorescence signal increased immediately and remained stable for the next 30 min (Figure 3B, C). For the CN-Es1 sensor, based on the fluorescence signal at 20 min, the linear range was 10 nM to 200 nM (inset of Figure 3C). The limit of detection (LOD) was calculated to be 9.1 nM using 3σ/slope, whereas σ was the variation of the background signal. The apparent $K_d$ from the sensor data was 162 nM, which just doubled the $K_d$ from ITC. For the CN-

Es2 sensor (Figure 3E, F), the linear range was 5 nM to 100 nM (inset of Figure 3F), and the LOD was 3.3 nM. The apparent $K_d$ from the sensor data was 103 nM, about three times of the $K_d$ from ITC. Such a small increase in the apparent $K_d$ can explain the relatively high background fluorescence, since the quencher-labeled strand was not a strong competitor. These results demonstrated that the sensors responded to E2 with good sensitivity.

To rule out fluorescence increase due to the intrinsic fluorescence of E2, we followed the fluorescence of E2 without the sensors, and no time or E2 concentration dependent fluorescence change was observed under our excitation and emission settings (Figure S3). We then added E2 to another sensor using the adenosine aptamer,[50] which did not respond to E2 (Figure S4). Therefore, the observed fluorescence increase here was due to the strand displacement reaction instead of artifacts. Compared to some previously published aptasensors for E2 (Table S4), our sensors had similar LOD, but our aptamers were much shorter and our detection time was also shorter (20 min versus 40 min to several hours). In addition, we did not use any nanomaterial or signal amplification methods, which can drive up sensitivity, although they also make the detection more complex.

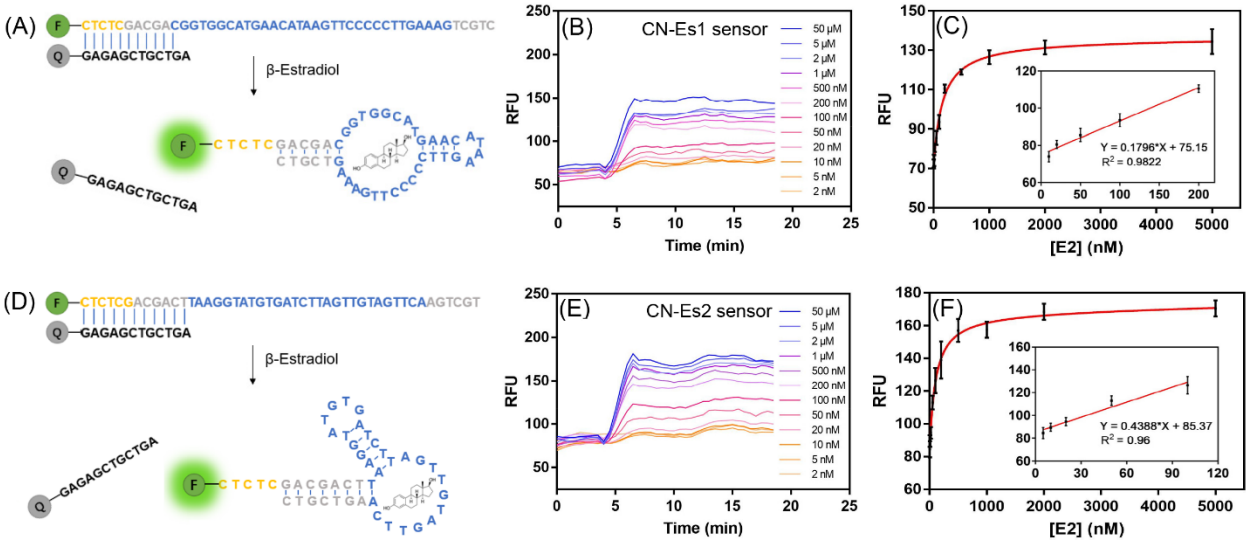



**Figure 3**. Aptamer-based fluorescent biosensors for the detection of E2. The schematic of (A) CN-Es1 and (D) CN-Es2 based sensors. Kinetic traces of 20 nM (B) CN-Es1 and (E) CN-Es2 sensors in the presence of various concentration of E2 ranging from 2 nM to 50 μM. E2 was added at ~4 min to the sensing buffer. Fluorescence intensity as a function of E2 concentration of (C) the CN-

Es1 sensor, and (F) the CN-Es2 sensor. Insets: the linear range and regression line at low E2 concentrations. The error bars indicate the standard deviation from three repetitions.

**Sensing estrogens as a group and E2 specifically**

For the selectivity test, 2 μM E2, its analogs, and other small molecules were respectively added to the CN-Es1 (Figure 4A) and CN-Es2 sensors (Figure 4B). The structures of these molecules are shown in Figure 4C. The $F/F_0$ value was used to evaluate the response. For the CN-Es1 sensor, E1 and EE2 also showed high $F/F_0$ values, demonstrating that aptamer CN-Es1 can bind to E1, E2 and EE2. Meanwhile, the other tested molecules had little response. We speculated that CN-Es1 binds to the common structure of these molecules in a way as shown in the orange lines in Figure 4C.

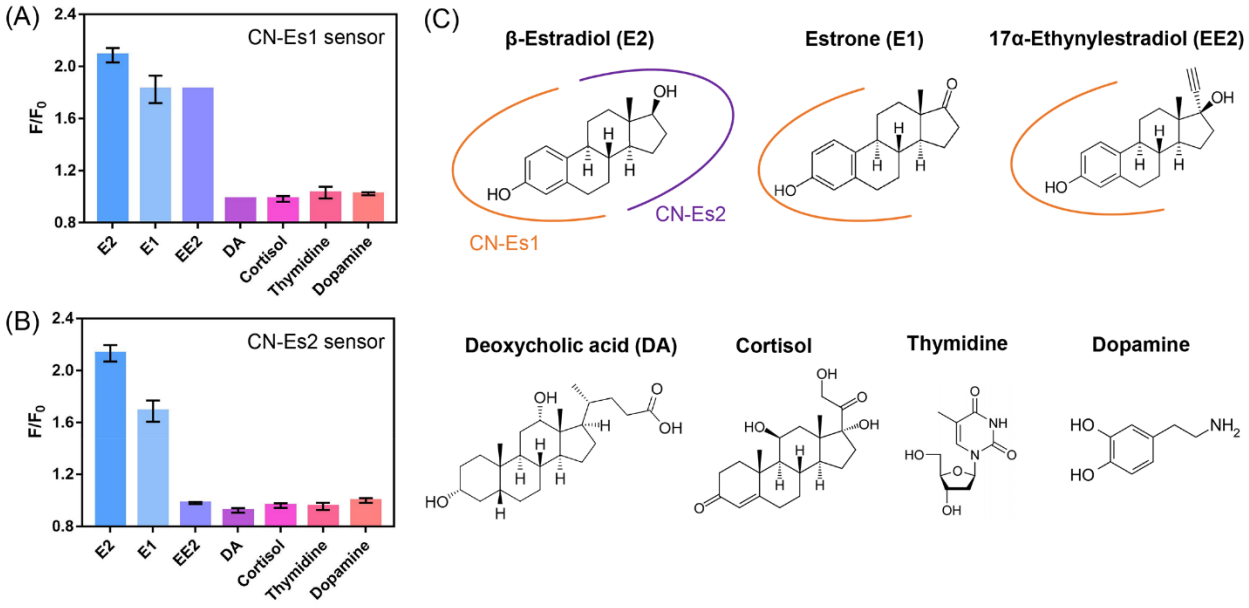



**Figure 4**. Specificity test of two biosensors with 2 μM E2 and other molecules: (A) the CN-Es1 sensor; and (B) the CN-Es2 sensors. The error bars indicate the standard deviation of three repetitions. (C) The structure of the molecules in the specificity test. The orange curve indicates a possible orientation of CN-Es1 aptamer binding to E2, and the purple curve indicates a possible way of CN-Es2 binding to E2.

For the CN-Es2 sensor, E2 showed the highest fluorescence enhancement followed by E1. Interestingly, EE2 showed no fluorescence increase. Therefore, compared to CN-Es1, CN-Es2 had better selectivity for E2. The selectivity for E2 over E1 is 5-fold based on their $K_d$ difference from ITC (Figure S5). Since E2 and E1 differ only by a hydrogen atom (a keto oxygen and a hydrogen group), this selectivity is reasonable. EE2 has an additional ethynyl group, which may pose a large steric hindrance in the aptamer binding pocket, leading to poor binding. Based on the selectivity, we proposed that CN-Es2 binds to E2 in a way shown by the purple line in Figure 4C.

For both aptamers, some other less related molecules such as cortisol, deoxycholic acid, thymidine, and dopamine showed no response. We reason that both aptamers are useful for environmental analytical chemistry. The CN-Es1 aptamer can detect the three estrogens as a group, while CN-Es2 shows better selectivity towards E2.

**Metal-dependent binding of E2**

Since environmental water samples may have various types and concentrations of metal ions, it is important to understand the requirement of metal ions for aptamer binding and sensing. Our typical sensing buffer contained 100 mM $Na^+$ and 10 mM $Mg^{2+}$. We first added 0.1 mM $Ca^{2+}$, $Mn^{2+}$ or $Zn^{2+}$ as potential interfering metal ions, and both sensors worked similarly (Figure S6), indicating that the sensors were not interfered by them. We then fully removed $Na^+$ from the sensing buffer, which did not affect the detection either. Finally, after removing $Mg^{2+}$ from the sensing buffer, neither the CN-Es1 nor the CN-Es2 sensor responded to E2. Therefore, both aptamers required $Mg^{2+}$ for E2 binding. The need for $Mg^{2+}$ was also confirmed by ITC (Figure S7).

**Detection of E2 in Wastewater**

To evaluate the aptamers in real environmental water samples, we further challenged our sensors with wastewater samples, which was very turbid and colored (Figure 5A). After allowing the samples to sit still for 24 h, the supernatant became clear and the large particles precipitated. We then collected the supernatant to test the sensors by spiking various concentrations of E2. We tested the selectivity of the two sensors in the wastewater samples and similar results as that in buffer were also achieved (Figure 5B, 5C). Based on the fluorescence signal at 20 min, the linear ranges of the two sensors were 10 nM to 100 nM (Figure 5D, 5E). The results indicated that our aptamers can bind to E2 in very challenging environmental water samples. Due to the high sensitivity of

fluorescence, it is also possible to detect them using a portable fluorometer[52] or other portable devices.[53-55]

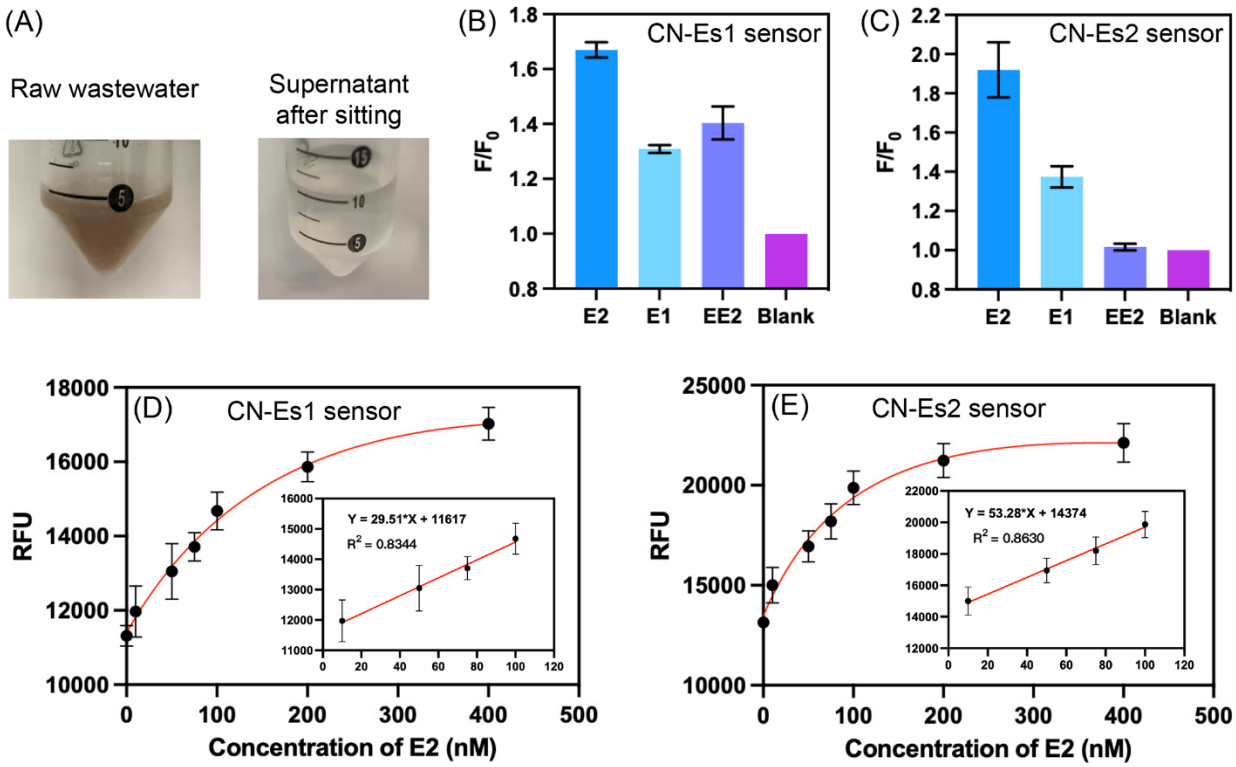



**Figure 5.** (A) Photograph of the raw wastewater sample and the supernatant after sitting for 24 h. Selectivity of the (B) CN-Es1 and (C) CN-Es2 sensors to 200 nM estrogens in the wastewater supernatant samples. Sensitivity of the (D) CN-Es1 and (E) CN-Es2 sensors in the wastewater sample.

## Comparison with Other Reported E2 Aptamers

As mentioned in the introduction part of this work, at least six previous DNA aptamer selections for E2 were reported by different research groups.[24, 28, 30-33] The two most commonly used E2 aptamers in designing biosensors were a 76-mer aptamer (Gu group),[24] and a 75-mer aptamer (Hodgkiss group).[28] In this work, we called them 76-mer-G and 75-mer-H, respectively. The E2Apt1 is an 84-mer sequence,[31] the aptamers reported by Vanschoenbeek et al were around 80-mer (Apta6A being a representative sequence),[30] the E28 is an 89-mer sequence,[32] while the BES.1

is a short 43-mer sequence.[33] We aligned all these six aptamers along with our CN-Es1 to CN-Es5 sequences using Clustal Omega (Figure 6A). The overall alignment was poor, suggesting that these sequences were not much related. A closer look at the sequences revealed that the 75-mer-H and E2Apt1 had the most similarity (Figure S8), although the majority of their similar nucleotides were in the constant primer binding regions of the libraries.

After analyzing their primary sequences, we then compared their secondary structures (Figure 6B-G). Based on DMF footprinting, the E2Apt1 aptamer has some of the E2 protected guanines in the structureless regions (e.g., G54 in Figure 6B), making it difficult to perform truncation.[31] The E28 aptamer contained multiple hairpin structures, but no truncated E28 aptamers were reported so far (Figure 6E). Thus, we did not study these two aptamers further. While a systematic truncation study was recently performed for the 76-mer-G aptamer using a gold nanoparticle based assay,[27] the optimal sequence named E09 was from nucleotide 58 to 72 (Figure 6C), which likely belong to the constant primer binding region instead of the random region. So, this is unlikely to be a successful truncation study and gold nanoparticles are known to be susceptible to artifacts in such assays.[56] The truncation of the 75-mer-H aptamer seems to be reasonable (Figure 6D), since the truncated 22-mer folds into a discernible hairpin structure. BES.1 aptamer was already truncated down to 43-mer folding in a three-way junction structure (Figure 6F). Finally, Apta6A forms a three-way junction and is a very long sequence (Figure 6G).

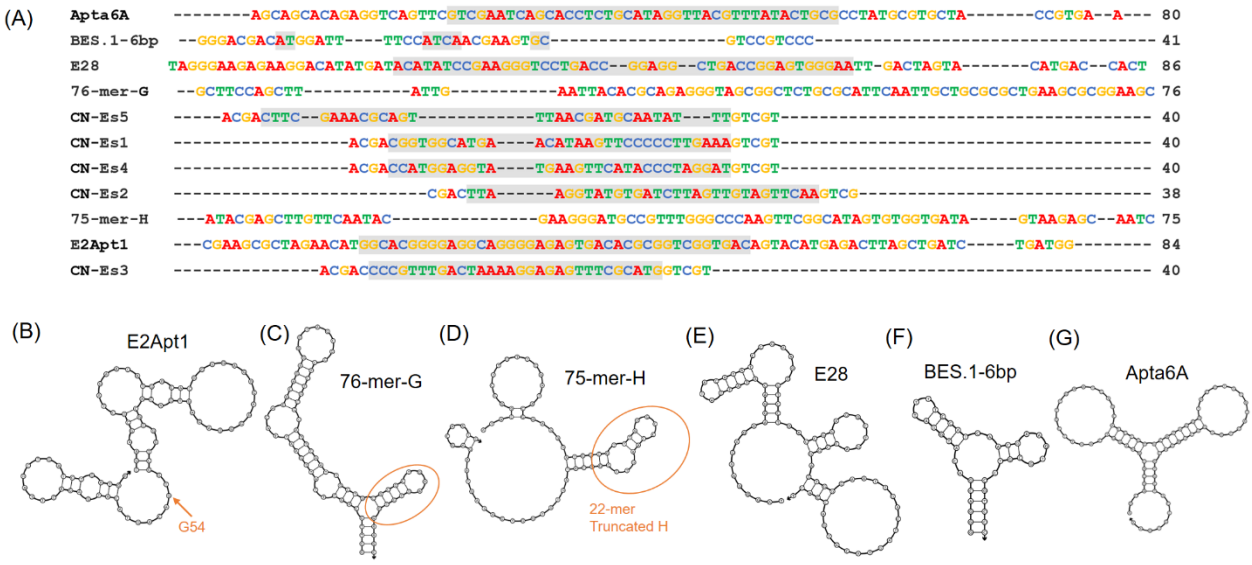



**Figure 6**. (A) Alignment of the six previously reported E2 aptamers and the CN-Es1 to CN-Es5 sequences from this work. The nucleotides from the random regions are highlighted in gray (if

reported). (B-G) The secondary structure of the six previously reported E2 aptamers. The orange circles indicate the truncated aptamers reported in the literature.

In 2017, the O'Sullivan group did a comprehensive comparison of binding assays of four E2 aptamers (76-mer-G, 75-mer-H, Apta6A and E2Apt1) using microscale thermophoresis, surface plasmon resonance and PCR.[57] For most of the assays, the full-length aptamers were used, and the general conclusion was that the measured $K_d$ values matched with the previously reported values. Therefore, in our current work, we focused on truncated aptamers, which are more desirable for biosensor design.

We compared E09 (truncated from 76-mer-G), 22-mer-truncated-H (from 75-mer-H) and BES.1. Their secondary structures are shown in Figure 7A-C. Then ITC was performed by titrating E2 into them in their respectively reported buffers. For E09, no heat change was observed (Figure 7D). This is not surprising since E09 is unlikely to be a viable truncated structure as it is in the primer binding region.[27] Similarly, no heat was observed for 22-mer-truncated-H (Figure 7E). This truncation was also based on gold nanoparticles,[29] which could be susceptible to artifacts such as target adsorption.[56]

For the BES.1 aptamer, an exothermic binding reaction was observed (Figure 7F), and the $K_d$ was calculated to be 1.1 ± 0.4 μM using a one-site binding model. It indicated that the BES.1 has 13-fold and 37-fold weaker binding compared to CN-Es1 and CN-Es2 respectively. Since the BES.1 library was pre-structured to fold in a three-way junction with only 8 randomized nucleotides, it is understandable that the binding was suboptimal.[34] Therefore, for the truncated aptamers, only BES.1 (43-mer) and our newly selected aptamers (38-40 mer) showed binding. All the other aptamers were longer than 75-mer with complex secondary structures. Overall, the new aptamers reported in this work have the combined advantages of being short and having high binding affinities.

As shown in Table 1, BES.1 has a binding stoichiometry greater than 2, suggesting the possibility of binding multiple E2 molecules. In addition, it has a large positive entropy change. In fact, the $T\Delta S$ term contribution to its binding was even greater than the enthalpy term, suggesting that its

binding was driven by entropy and likely hydrophobic interactions (e.g. release of associated water molecules to increase the system's entropy as a way of enhancing binding).

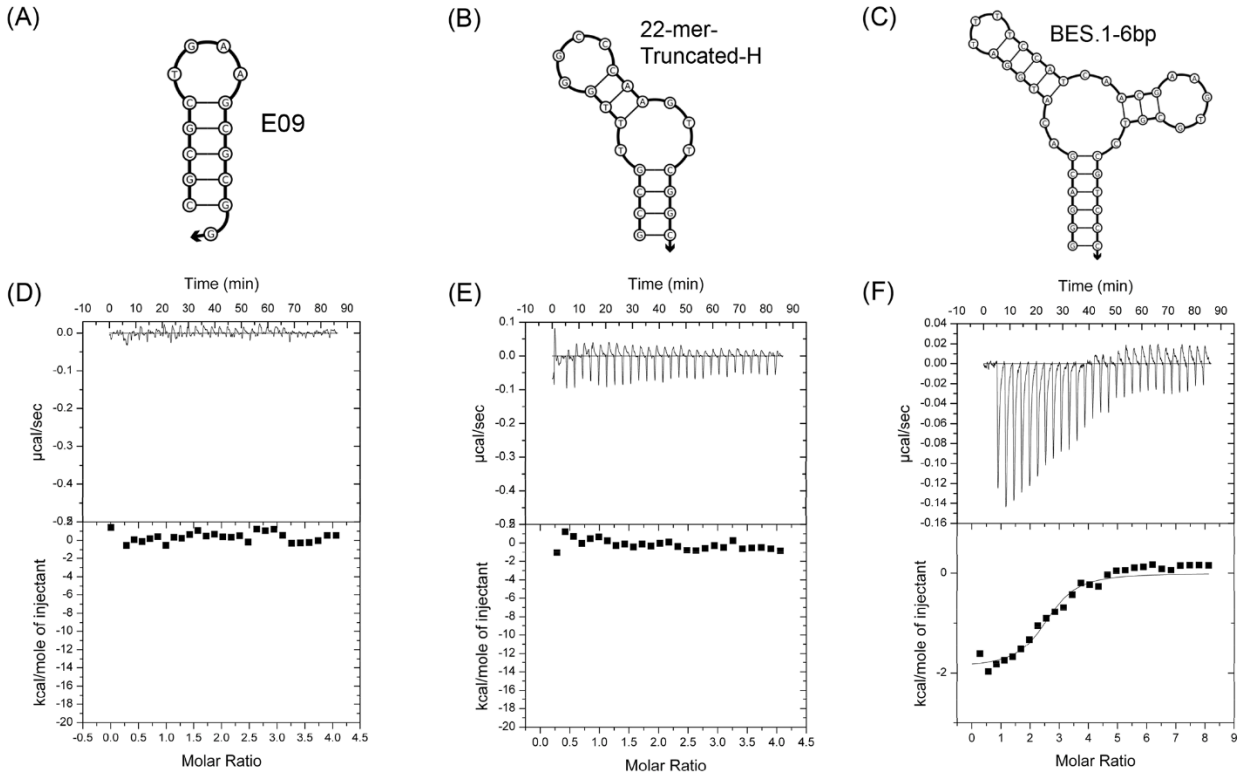



**Figure 7**. The secondary structure of the three previously reported truncated E2 aptamers: (A) E09; (B) 22-mer-truncated-H, and (C) BES.1. The arrows indicates the 3′-ends. The ITC data of the aptamers in their respective selection buffers: (D) E09, (E) 22-mer-truncated-H, and (F) BES.1.

## Discussion

While at least six DNA aptamer selections were previously reported using E2 as the target, a careful analysis revealed that those aptamers were either too long, difficult to truncate, or with low to no binding affinities after truncation. In addition, the majority of the selections were performed by using immobilized E2 molecules, which may hinder optimal aptamer binding to the free target. In this work, we selected new aptamers by using an immobilized and fully random DNA library and free E2. Using ITC to verify the binding, the $K_d$ values were from 30 nM to 157 nM for the

most abundant three aptamers. For the specificity, CN-Es1 has a similar affinity to the three estrogens. CN-Es2 bound to E2 with the highest affinity, but showed no response to EE2.

We developed two aptamer-based structure-switching fluorescent biosensors for the detection of E2 with the LOD down to 3.3 nM. In addition, wastewater was tested and the sensors could also work in this very challenging sample, highlighting the high stability of DNA. Future work to use these aptamers can be focused on the extraction of E2 from water, such as the packing the aptamers on a column and the development of portable detection systems for on-site detection. The feasibility of using aptamers for in vivo analysis such as E2 in fish tissues is also a topic of great environmental interest.[58]

Finally, we compared our aptamers with all the previously reported ones using primary sequence alignment and secondary structure analysis. Using ITC, we compared all the E2 aptamers with reported truncated sequences. Only one of them showed a $K_d$ of 1.1 μM, while the rest two did not bind. Therefore, our newly selected aptamers have the combined advantage of small size and high affinity. Given the importance of E2 in environmental chemistry, our new aptamers will find applications in the extraction and detection of E2 and related compounds.

## Conflicts of interest

There are no conflicts to declare


## Acknowledgements

Funding for this work was from the Natural Sciences and Engineering Research Council of Canada (NSERC). C. Niu was supported by a China Scholarship Council (CSC) scholarship to visit the University of Waterloo.


## Supporting Information

The Supporting Information is available free of charge.

DNA sequences used in this work (Table S1). Selection conditions (Table S2). The proportion of CN-Es1 to 5 in each round (Table S3). Comparison of fluorescent aptamer biosensors (Table S4). The SELEX scheme used in this study (Figure S1). Using real-time PCR to monitor the progress of the selection (Figure S2). The verification of the feasibility of the sensor (Figure S3 and S4). The ITC data of the binding of E1 and EE2 (Figure S5). The effect of different metal ions in samples on binding (Figure S6). ITC data of aptamer binding without $Mg^{2+}$ (Figure S7). Alignment of the aptamers 75-mer-H and E2Apt1 (Figure S8).

## References


(1) Hall, J. M.; Couse, J. F.; Korach, K. S., The Multifaceted Mechanisms of Estradiol and Estrogen Receptor Signaling. *J. Biol. Chem.* **2001**, 276, 36869-36872.

(2) Adeel, M.; Song, X.; Wang, Y.; Francis, D.; Yang, Y., Environmental Impact of Estrogens on Human, Animal and Plant Life: A Critical Review. *Environ. Int.* **2017**, 99, 107-119.

(3) Hanselman, T. A.; Graetz, D. A.; Wilkie, A. C., Manure-Borne Estrogens as Potential Environmental Contaminants: A Review. *Environ. Sci. Technol.* **2003**, 37, 5471-5478.

(4) Kidd, K. A.; Blanchfield, P. J.; Mills, K. H.; Palace, V. P.; Evans, R. E.; Lazorchak, J. M.; Flick, R. W., Collapse of a Fish Population after Exposure to a Synthetic Estrogen. *Proc. Natl. Acad. Sci. USA* **2007**, 104, 8897-8901.

(5) Regal, P.; Seijas, J. A.; Cepeda, A.; Fente, C., Structure Elucidation and HPLC-MS/MS Determination of a Potential Biomarker for Estradiol Administration in Cattle. *Anal. Bioanal. Chem.* **2013**, 405, 9537-9546.

(6) Denver, N.; Khan, S.; Homer, N. Z. M.; MacLean, M. R.; Andrew, R., Current Strategies for Quantification of Estrogens in Clinical Research. *J. Steroid Biochem. Mol. Biol.* **2019**, 192, 105373.

(7) Spychalska, K.; Zając, D.; Cabaj, J., Electrochemical Biosensor for Detection of 17β-Estradiol Using Semi-Conducting Polymer and Horseradish Peroxidase. *RSC Adv.* **2020**, 10, 9079-9087.

(8) Wang, A.; Ding, Y.; Li, L.; Duan, D.; Mei, Q.; Zhuang, Q.; Cui, S.; He, X., A Novel Electrochemical Enzyme Biosensor for Detection of 17β-Estradiol by Mediated Electron-Transfer System. *Talanta* **2019**, 192, 478-485.

(9) Povedano, E.; Cincotto, F. H.; Parrado, C.; Díez, P.; Sánchez, A.; Canevari, T. C.; Machado, S. A. S.; Pingarrón, J. M.; Villalonga, R., Decoration of Reduced Graphene Oxide with Rhodium Nanoparticles for the Design of a Sensitive Electrochemical Enzyme Biosensor for 17β-Estradiol. *Biosens. Bioelectron.* **2017**, 89, 343-351.

(10) Zhang, G.; Li, T.; Zhang, J.; Chen, A., A Simple Fret-Based Turn-on Fluorescent Aptasensor for 17β-Estradiol Determination in Environmental Water, Urine and Milk Samples. *Sens. Actuators B Chem.* **2018**, 273, 1648-1653.

(11) Zhu, J.-H.; Wang, M.; Tu, L.-H.; Wang, A.-J.; Luo, X.; Mei, L.-P.; Zhao, T.; Feng, J.-J., Nanosheets-Assembled Hollow $CdIn_2S_4$ Microspheres-Based Photoelectrochemical and

Fluorescent Dual-Mode Aptasensor for Highly Sensitive Assay of 17β-Estradiol Based on Magnetic Separation and Enzyme Catalytic Amplification. *Sens. Actuators B Chem.* **2021**, 347, 130553.
(12) Zhang, D.; Zhang, W.; Ye, J.; Zhan, S.; Xia, B.; Lv, J.; Xu, H.; Du, G.; Wang, L., A Label-Free Colorimetric Biosensor for 17β-Estradiol Detection Using Nanoparticles Assembled by Aptamer and Cationic Polymer. *Aust. J. Chem.* **2015**, 69, 12-19.
(13) Minopoli, A.; Sakač, N.; Lenyk, B.; Campanile, R.; Mayer, D.; Offenhäusser, A.; Velotta, R.; Della Ventura, B., Lspr-Based Colorimetric Immunosensor for Rapid and Sensitive 17β-Estradiol Detection in Tap Water. *Sens. Actuators B Chem.* **2020**, 308, 127699.
(14) Chang, C.-C.; Yeh, C.-Y., Using Simple-Structured Split Aptamer for Gold Nanoparticle-Based Colorimetric Detection of Estradiol. *Anal. Sci.* **2020**, 20SCP07.
(15) Nezami, A.; Nosrati, R.; Golichenari, B.; Rezaee, R.; Chatzidakis, G. I.; Tsatsakis, A. M.; Karimi, G., Nanomaterial-Based Aptasensors and Bioaffinity Sensors for Quantitative Detection of 17β-Estradiol. *TrAC Trends Anal. Chem.* **2017**, 94, 95-105.
(16) Long, F.; Shi, H.; Wang, H., Fluorescence Resonance Energy Transfer Based Aptasensor for the Sensitive and Selective Detection of 17β-Estradiol Using a Quantum Dot-Bioconjugate as a Nano-Bioprobe. *RSC Adv.* **2014**, 4, 2935-2941.
(17) Dou, M.; García, J. M.; Zhan, S.; Li, X., Interfacial Nano-Biosensing in Microfluidic Droplets for High-Sensitivity Detection of Low-Solubility Molecules. *Chem. Commun.* **2016**, 52, 3470-3473.
(18) Tao, X.; Peng, Y.; Liu, J., Nanomaterial-Based Fluorescent Biosensors for Veterinary Drug Detection in Foods. *J. Food Drug Anal.* **2020**, 28, 575-594.
(19) Yu, H.; Alkhamis, O.; Canoura, J.; Liu, Y.; Xiao, Y., Advances and Challenges in Small-Molecule DNA Aptamer Isolation, Characterization, and Sensor Development. *Angew. Chem. Int. Ed.* **2021**, 60, 16800-16823.
(20) Wu, L.; Wang, Y.; Xu, X.; Liu, Y.; Lin, B.; Zhang, M.; Zhang, J.; Wan, S.; Yang, C.; Tan, W., Aptamer-Based Detection of Circulating Targets for Precision Medicine. *Chem. Rev.* **2021**, 121, 12035-12105.
(21) Nakatsuka, N.; Yang, K.-A.; Abendroth, J. M.; Cheung, K. M.; Xu, X.; Yang, H.; Zhao, C.; Zhu, B.; Rim, Y. S.; Yang, Y.; Weiss, P. S.; Stojanović, M. N.; Andrews, A. M., Aptamer–Field-Effect Transistors Overcome Debye Length Limitations for Small-Molecule Sensing. *Science* **2018**, 362, 319-324.
(22) Wang, R.; Chon, H.; Lee, S.; Cheng, Z.; Hong, S. H.; Yoon, Y. H.; Choo, J., Highly Sensitive Detection of Hormone Estradiol E2 Using Surface-Enhanced Raman Scattering Based Immunoassays for the Clinical Diagnosis of Precocious Puberty. *ACS Appl. Mater. Interfaces* **2016**, 8, 10665-10672.
(23) McConnell, E. M.; Nguyen, J.; Li, Y., Aptamer-Based Biosensors for Environmental Monitoring. *Front. Chem.* **2020**, 8, 434.
(24) Kim, Y. S.; Jung, H. S.; Matsuura, T.; Lee, H. Y.; Kawai, T.; Gu, M. B., Electrochemical Detection of 17β-Estradiol Using DNA Aptamer Immobilized Gold Electrode Chip. *Biosens. Bioelectron.* **2007**, 22, 2525-2531.
(25) Wang, W.; Peng, Y.; Wu, J.; Zhang, M.; Li, Q.; Zhao, Z.; Liu, M.; Wang, J.; Cao, G.; Bai, J.; Gao, Z., Ultrasensitive Detection of 17β-Estradiol (E2) Based on Multistep Isothermal Amplification. *Anal. Chem.* **2021**, 93, 4488-4496.

(26) Ming, T.; Wang, Y.; Luo, J.; Liu, J.; Sun, S.; Xing, Y.; Xiao, G.; Jin, H.; Cai, X., Folding Paper-Based Aptasensor Platform Coated with Novel Nanoassemblies for Instant and Highly Sensitive Detection of 17β-Estradiol. *ACS Sens.* **2019**, 4, 3186-3194.
(27) Qiao, L.; Wang, H.; He, J.; Yang, S.; Chen, A., Truncated Affinity-Improved Aptamers for 17β-Estradiol Determination by Aunps-Based Colorimetric Aptasensor. *Food Chem.* **2021**, 340, 128181.
(28) Alsager, O. A.; Kumar, S.; Willmott, G. R.; McNatty, K. P.; Hodgkiss, J. M., Small Molecule Detection in Solution Via the Size Contraction Response of Aptamer Functionalized Nanoparticles. *Biosens. Bioelectron.* **2014**, 57, 262-268.
(29) Alsager, O. A.; Kumar, S.; Zhu, B.; Travas-Sejdic, J.; McNatty, K. P.; Hodgkiss, J. M., Ultrasensitive Colorimetric Detection of 17β-Estradiol: The Effect of Shortening DNA Aptamer Sequences. *Anal. Chem.* **2015**, 87, 4201-4209.
(30) Vanschoenbeek, K.; Vanbrabant, J.; Hosseinkhani, B.; Vermeeren, V.; Michiels, L., Aptamers Targeting Different Functional Groups of 17β-Estradiol. *J. Steroid Biochem. Mol. Biol.* **2015**, 147, 10-16.
(31) Akki, S. U.; Werth, C. J.; Silverman, S. K., Selective Aptamers for Detection of Estradiol and Ethynylestradiol in Natural Waters. *Environ. Sci. Technol.* **2015**, 49, 9905-9913.
(32) Jauset-Rubio, M.; Botero, M. L.; Skouridou, V.; Aktas, G. l. B. l.; Svobodova, M.; Bashammakh, A. S.; El-Shahawi, M. S.; Alyoubi, A. O.; O'Sullivan, C. K., One-Pot Selex: Identification of Specific Aptamers against Diverse Steroid Targets in One Selection. *ACS Omega* **2019**, 4, 20188-20196.
(33) Yang, K.-A.; Pei, R.; Stefanovic, D.; Stojanovic, M. N., Optimizing Cross-Reactivity with Evolutionary Search for Sensors. *J. Am. Chem. Soc.* **2012**, 134, 1642-1647.
(34) Yang, K.-A.; Chun, H.; Zhang, Y.; Pecic, S.; Nakatsuka, N.; Andrews, A. M.; Worgall, T. S.; Stojanovic, M. N., High-Affinity Nucleic-Acid-Based Receptors for Steroids. *ACS Chem. Biol.* **2017**, 12, 3103-3112.
(35) Xu, D.; Chatakonda, V.-K.; Kourtidis, A.; Conklin, D. S.; Shi, H., In Search of Novel Drug Target Sites on Estrogen Receptors Using RNA Aptamers. *Nucleic Acid Ther.* **2014**, 24, 226-238.
(36) Musa, A. M.; Kiely, J.; Luxton, R.; Honeychurch, K. C., Recent Progress in Screen-Printed Electrochemical Sensors and Biosensors for the Detection of Estrogens. *TrAC Trends Anal. Chem.* **2021**, 139, 116254.
(37) Liu, S. Y.; Wang, Z. M.; Chen, Y. Q.; Cao, T. C.; Zhao, G. H., Recognition and Selectivity Analysis Monitoring of Multicomponent Steroid Estrogen Mixtures in Complex Systems Using a Group-Targeting Environmental Sensor. *Environ. Sci. Technol.* **2021**, 55, 14115-14125.
(38) Li, Y.; Zhu, Y.; Wang, C.; He, M.; Lin, Q., Selective Detection of Water Pollutants Using a Differential Aptamer-Based Graphene Biosensor. *Biosens. Bioelectron.* **2019**, 126, 59-67.
(39) Wang, X.; Pei, K. L.; Sun, H. Y.; Wang, Q., A Magnetic Relaxation Switch Sensor for Determination of 17 Beta-Estradiol in Milk and Eggs Based on Aptamer-Functionalized Fe-$O_4$@Au Nanoparticles. *J. Sci. Food Agric.* **2021**, 101, 5697-5706.
(40) Suo, T. Y.; Sohail, M.; Ma, Y. J.; Li, B. Z.; Chen, Y.; Zhang, X.; Zhou, X. M., A Versatile Turn-on Fluorometric Biosensing Profile Based on Split Aptamers-Involved Assembly of Nanocluster Beacon Sandwich. *Sens. Actuators B Chem.* **2020**, 324, 128586.
(41) Yang, K.-A.; Pei, R.; Stojanovic, M. N., In Vitro Selection and Amplification Protocols for Isolation of Aptameric Sensors for Small Molecules. *Methods* **2016**, 106, 58-65.

(42) Huang, P.-J. J.; Liu, J., Selection of Aptamers for Sensing Caffeine and Discrimination of Its Three Single Demethylated Analogues. *Anal. Chem.* **2022**, 94, 3142-3149.
(43) Niu, C.; Ding, Y.; Zhang, C.; Liu, J., Comparing Two Cortisol Aptamers for Label-Free Fluorescent and Colorimetric Biosensors. *Sens. Diagn.* **2022,** 1, 541-549.
(44) Nutiu, R.; Li, Y., In Vitro Selection of Structure-Switching Signaling Aptamers. *Angew. Chem. Int. Ed.* **2005**, 44, 1061-1065.
(45) Yu, H.; Luo, Y.; Alkhamis, O.; Canoura, J.; Yu, B.; Xiao, Y., Isolation of Natural DNA Aptamers for Challenging Small-Molecule Targets, Cannabinoids. *Anal. Chem.* **2021**, 93, 3172-3180.
(46) Lyu, C.; Khan, I. M.; Wang, Z., Capture-Selex for Aptamer Selection: A Short Review. *Talanta* **2021**, 229, 122274.
(47) Luo, Y.; Jin, Z.; Wang, J.; Ding, P.; Pei, R., The Isolation of a DNA Aptamer to Develop a Fluorescent Aptasensor for the Thiamethoxam Pesticide. *Analyst* **2021**, 146, 1986-1995.
(48) Jenison, R. D.; Gill, S. C.; Pardi, A.; Polisky, B., High-Resolution Molecular Discrimination by RNA. *Science* **1994**, 263, 1425-1429.
(49) Liu, Y.; Liu, J., Selection of DNA Aptamers for Sensing Uric Acid in Simulated Tears. *Anal. Sens.* **2022**, 2, e202200010.
(50) Nutiu, R.; Li, Y., Structure-Switching Signaling Aptamers. *J. Am. Chem. Soc.* **2003**, 125, 4771-4778.
(51) Huang, P.-J. J.; Liu, J., A DNA Aptamer for Theophylline with Ultrahigh Selectivity Reminiscent of the Classic RNA Aptamer. *ACS Chem. Biol.* **2022**, 17, 2121–2129.
(52) Lake, R. J.; Yang, Z. L.; Zhang, J. L.; Lu, Y., Dnazymes as Activity-Based Sensors for Metal Ions: Recent Applications, Demonstrated Advantages, Current Challenges, and Future Directions. *Acc. Chem. Res.* **2019**, 52, 3275-3286.
(53) Yildirim, N.; Long, F.; He, M.; Gao, C.; Shi, H.-C.; Gu, A. Z., A Portable DNAzyme-Based Optical Biosensor for Highly Sensitive and Selective Detection of Lead (II) in Water Sample. *Talanta* **2014**, 129, 617-622.
(54) Zhao, Y.; Yavari, K.; Wang, Y.; Pi, K.; Van Cappellen, P.; Liu, J., Deployment of Functional DNA-Based Biosensors for Environmental Water Analysis. *TrAC Trends Anal. Chem.* **2022**, 153, 116639.
(55) Ross, S.; Wu, R. S.; Wei, S. C.; Ross, G. M.; Chang, H. T., The Analytical and Biomedical Applications of Carbon Dots and Their Future Theranostic Potential: A Review. *J. Food Drug Anal.* **2020**, 28, 677-695.
(56) Zhang, F.; Liu, J., Label-Free Colorimetric Biosensors Based on Aptamers and Gold Nanoparticles: A Critical Review. *Anal. Sens.* **2021**, 1, 30-43.
(57) Svobodová, M.; Skouridou, V.; Botero, M. L.; Jauset-Rubio, M.; Schubert, T.; Bashammakh, A. S.; El-Shahawi, M. S.; Alyoubi, A. O.; O'Sullivan, C. K., The Characterization and Validation of 17β-Estradiol Binding Aptamers. *J. Steroid Biochem. Mol. Biol.* **2017**, 167, 14-22.
(58) Roszkowska, A.; Yu, M.; Bessonneau, V.; Ings, J.; McMaster, M.; Smith, R.; Bragg, L.; Servos, M.; Pawliszyn, J., In vivo Solid-Phase Microextraction Sampling Combined with Metabolomics and Toxicological Studies for the Non-Lethal Monitoring of the Exposome in Fish Tissue. *Environ. Pollut.* **2019**, 249, 109-115.

579

580

581 For TOC graphics only

582 